Zibaei *et al. Cancer Nano* (2021) 12:3
https://doi.org/10.1186/s12645-020-00074-4

Cancer Nanotechnology

RESEARCH Open Access

Curcumin-enriched Gemini surfactant nanoparticles exhibited tumoricidal effects on human 3D spheroid HT-29 cells in vitro

Zohre Zibaei[1†], Esmaeil Babaei[1,2*†], Arezoo Rezaie Nezhad Zamani[3], Reza Rahbarghazi[3,4*†] and Hewa Jalal Azeez[1]

*Correspondence: babaei@tabrizu.ac.ir; rezarahbardvm@gmail.com; rahbarghazir@tbzmed.ac.ir
†Esmaeil Babaei and Reza Rahbarghazi contributed equally to this work
[1] Department of Animal Biology, School of Natural Sciences, University of Tabriz, Tabriz 51555, Iran
[4] Department of Applied Cell Sciences, Faculty of Advanced Medical Sciences, Tabriz University of Medical Sciences, Golgasht St., Tabriz 5166614756, Iran
Full list of author information is available at the end of the article

Abstract

Background: Here, we examined the tumoricidal effect of Gemini surfactant nanoparticles enriched with curcumin on 3D spheroid HT-29 cells. The delivery of curcumin and other phytocompounds to the tumor niche is an important challenge.

Methods: Spheroid HT-29 cells were generated by using a conventional hanging drop method and exposed to different concentrations of Gemini-curcumin nanoparticles. The changes in spheroid integrity and cell viability were evaluated by measuring the spheroid diameter and LDH release, respectively. The uptake of Gemini-curcumin nanoparticles was detected by flow cytometry assay. Flow cytometric of Rhodamine 123 efflux was also performed. Migration capacity was analyzed using a Transwell insert assay. By using real-time PCR analysis and Western blotting, we studied the expression level of MMP-2, -9, Vimentin, and E-cadherin genes.

Results: Gemini-curcumin nanoparticles had the potential to disintegrate spheroids and decrease central density compared to the control group ($p < 0.05$). These changes coincided with enhanced LDH release by the increase of nanoparticle concentration ($p < 0.05$). Data highlighted the ability of cells to uptake synthetic nanoparticles in a dose-dependent manner. We found reduced Rhodamine 123 efflux in treated HT-29 spheroid cells compared to the control ($p < 0.05$). Nanoparticles significantly decreased the metastasis and epithelial-mesenchymal transition (EMT) rate by the suppression of MMP-2 and MMP-9, Vimentin, and induction of E-cadherin ($p < 0.05$).

Conclusion: Our data confirmed that Gemini curcumin has the potential to suppress cell proliferation and inhibit metastasis in 3D spheroid HT-29 cells in vitro.

Keywords: Curcumin, Gemini surfactants, 3D spheroid culture, HT-29, Colorectal cancer

Background

Colorectal cancer (CRC) is considered a manifold life-threatening diseases globally affecting both females and males (Rawla et al. 2019). Annually, numerous patients have died due to the lack of CRC development and metastasis. Therefore, it is imperative to develop novel treatments and modalities to put a halt to CRC development and dire

consequences (Pretzsch et al. 2019). Despite various treatment modalities available in human medicine, phytomedicine is considered as an alternative approach to circumvent side effects correlated with conventional therapies (Cheraghi et al. 2016). Phytomedicine is an herbal-based traditional medical practice that uses various plant materials for both prevention and therapeutic purposes (Chaudhary et al. 2015). Curcumin (Cur) is one of the herbal compounds that possess anti-cancer properties without magnificent side effects (Rahnavard et al. 2019). From a structural point of view, Cur is a polyphenol commonly extracted from the rhizomes of *Curcuma longa* L. In traditional medicine, Cur is prescribed as anti-oxidant, anti-inflammatory, anti-carcinogenic, and chemopreventive agents (Wang et al. 2009). It has been elucidated that the anti-cancer effect of Cur is mediated by the modulation of multiple signaling pathways, such as Wnt/β-catenin, MAPK, PI3K/Akt, p53, JAK/STAT, and NF-dB (Wang et al. 2019; Chauhan et al. 2018; Srivastava and Srivastava 2019). Due to these advantages, Cur has grabbed the researchers' attention in the field of cancer biology research and treatment (Vallianou et al. 2015; Hewlings and Kalman 2017). Despite the undeniable advantages, some studies declared that Cur possesses poor bio-distribution and absorption rate after oral intake (Karimpour et al. 2019).

The development of a lipid-based delivery system is an alternative approach to increase the bioavailability of hydrophobic components, like Cur, to the target tissues (Nayak et al. 2016). The application of nanoparticles and physicochemical modification seems logical to increase the distribution rate in the in vivo milieu (Lee et al. 2013; Shome et al. 2016; Rahimi et al. 2016). In this regard, Gemini surfactants, belonging to a surfactant family with two identical surfactants, are linked by a flexible or rigid spacer that could harbor and deliver many compounds to the target sites (Karimpour et al. 2019). Unlike traditional surfactants, the use of a spacer in Gemini surfactants can connect two hydrophilic groups by chemical bonds to form a structure with double hydrophilic groups and double hydrophobic chains. The current configuration dedicates far more merits, including higher surface tension, higher micelle forming ability, and better water solubility (Du et al. 2018). Notably, very low concentrations of Gemini surfactants are sufficient to form spheroidal micelles without toxicity to the host cells. These features make Gemini nanoparticles eligible for the delivery of drugs, proteins, and genetic factors (Karimpour et al. 2019). Besides, the stereochemistry of the Gemini surfactant leads to specific potential features compared to other carrier liposomes and PEGylated lipoplexes. It seems that the fusion rate of Gemini surfactant and the cell membrane is high. These features facilitate the transfer of target molecules and intracellular distribution in host cells compared to other delivery systems mainly liposomes (Aleandri et al. 2013). The major hurdle of PEGylation is associated with the enlargement of whole nanoparticle size which limits the uptake and subcellular distribution (Sebak 2018).

In the most well-known experiments, the tumoricidal effects of Cur have been examined in different cancer cell lines in the 2D culture systems, which does not fully mimic the in vivo conditions of the cancerous niche (Nunes et al. 2019). In this line, the development of 3D cell cultures, such as spheroids and tumor organoids, could reflect the real growth dynamics and morphology of solid tumors. In the current research, Gemini-Cur (Cur-Gemini) is utilized as nano-formulations for delivering different concentrations of

Cur human colorectal carcinoma cells HT-29 (Karimpour et al. 2019; Du et al. 2018). It seems that the results from this study will help us understand the tumoricidal activity of Cur inside Gemini surfactants in a 3D culture system.

Material and methods

Synthesis of Gemini-Cur nanoparticles (NPs)

Synthesis

Curcumin-loaded NPs were synthesized by a single-step nano-precipitation method as previously described by our group. In brief, 6 mg of Cur (Cat no: Sigma-Aldrich, USA) and 100 mg of methoxyl-poly(ethylene glycol) urethane Gemini surfactant (provided as a gift from Institute for Color Science and Technology, Tehran, Iran) were dissolved in 5 ml of methanol solution (Merck). Then, the methanol was evaporated in a rotary evaporator. The Gemini-Cur NPs solution were filtered using a 0.2 μm size syringe filter (Millex-LG, Millipore Co., USA) to exclude the impurity and sterilize the solution Gemini-Cur NPs, were lyophilized, and stored at 4 °C until use. The characterization of Gemini-Cur NPs was done according to our previous study (Karimpour et al. 2019).

Fourier transforms infrared spectroscopy (FTIR) analysis

The conjugation of Cur with Gemini NPs was assessed using FTIR analysis (Bruker, Tensor 27 spectrophotometer, Germany). Samples from Cur, Gemini NPs, and Cur + Gemini NPs were prepared and mixed with KBr to generate pellets followed by compressing under high pressure. Samples were scanned at the range of 500 to 4500 $cm^{-1.}$

Scanning electron microscopy (SEM)

The diameters of Gemini-Cur NPs were measured by SEM (Model: MIRA3 FEG-SEM, Tescan) at a voltage of 5 kV. NPs were placed on the SEM stubs and visualized after sputter coating with gold.

Measuring Gemini-Cur NPs uptake using immunofluorescence imaging

To assess the uptake of Gemini-Cur NPs, we exposed HT-29 cells with 80 μM Gemini-Cur NPs for 6 h. To this end, 1×10^4 cells were plated in each well of 96-well plates and allowed to reach 70–80% confluence. Then, cells were incubated with Gemini-Cur NPs for 6 h followed by twice washes in PBS. Cells were fixed using 4% pre-cold paraformaldehyde solution for 20 min and visualized under fluorescence microscopy.

Cell culture protocol

In this study, human colorectal carcinoma cells HT-29 (NCBI Code: C466) were obtained from the National Cell Bank of Iran (Pasteur Institute, Tehran, Iran). To expand the cells, a high-content glucose DMEM (DMEM/HG; Gibco) culture medium was used. The basal medium was enriched with 10% fetal bovine serum (FBS, Gibco, USA) and 1% Pen-Strep solution (Biochrom GbmH, Berlin, Germany). Cells between passages 3–6 were subjected to different analyses.

MTT assay

Effect of Gemini-Cur NPs on human HT-29 cells viability in a 2D culture system

The viability of HT-29 cells in 2D monolayer culture was evaluated after treatment with Gemini-Cur NPs by using MTT (3-(4, 5-dimethylthiazole-2-yl)-2,5- diphenyltetrazolium bromide) method. For this purpose, an initial number of 1×10^4 cells were suspended in 100 mL of DMEM/HG containing 10% FBS and plated in each well of 96-well plates. Cells were allowed to reach an appropriate confluence. Cells were incubated with different concentrations of Gemini-Cur NPs for 48 h. After completion of the incubation period, supernatants were discarded and replaced with 5 mg/ml of MTT solution. Cells were kept at 37 ˚C for 3–4 h. Then, we added the DMSO solution to dissolve the formazan crystals. The OD of each group was read using a microplate reader and expressed as % of the control group.

Effect of Gemini-Cur NPs on human HT-29 cells spheroid integrity

To this end, cancer cell spheroids were generated using the conventional hanging drop method (Abdolahinia et al. 2019). Briefly, 1×10^4 HT-29 cells were re-suspended in 20 µl of culture medium containing 1% FBS and placed at the inner surface of culture plate lids. The lid and drop containing cells were inverted over the culture plates. The wells were filled with phosphate-buffered saline to inhibit the evaporation of hanging drops. The plates were kept at 37 °C under a humidified condition with 5% CO_2. By using the eyepiece of an inverted microscope, the spheroids were monitored. When thick and compact microaggregates with dark edges were generated, the spheroids were transferred into each well of 96-well plates containing 200 µl of culture medium with 1–2% FBS. The spheroids were incubated with different concentrations of Gemini-Cur NPs for 48 h. To evaluate the tumoricidal effect of Gemini-Cur NPs on HT-29 spheroids, we also measured the diameter using Image J software (NIH).

Lactate dehydrogenase (LDH) assay

The release of LDH to the supernatant culture medium exhibits the occurrence of cell membrane injury. To further confirm the cytotoxicity of Gemini-Cur NPs on HT-29 spheroids, supernatants were collected. The concentrations of LDH were measured using the LDH assay kit (Pars Azmun, Tehran, Iran) according to the manufacturer's instructions.

Analysis of Gemini-Cur NPs uptake using flow cytometry analysis

For this purpose, the spheroids were incubated with 80 and 300 µM Gemini-Cur NPs for 48 h. After completion of the treatment protocol, the culture medium was discarded. Spheroids were disaggregated by incubating in the Trypsin–EDTA solution. After blocking the enzymatic solution, the spheroids were gently triturated. The cells were washed twice with PBS solution and analyzed by the BD FACSCalibur system. The raw data were analyzed using FlowJo software (ver. 7.6.1). Finally, fluoresce intensity was measured in each group and compared to the non-treated control cells.

Rhodamine-123 (Rh-123) efflux

Rh-123 efflux assay was performed used to detect the functional activity MDR1/P-gp of cells after treatment with Gemini-Cur NPs. HT-29 spheroids were incubated with 80 and 300 μM Gemini-Cur NPs for 48 h. Thereafter, spheroids were incubated with Trypsin–EDTA solution and gently agitated to make a single-cell suspension. Cells were washed twice with PBS and incubated with 10 μg/ml of Rh-123 (Sigma-Aldrich) at 37 °C for 30–40 min. Then, cells were washed with PBS to exclude extra RH-123 solution. The cells were analyzed by flow cytometry and FlowJo software (Ver.7.6.1.).

Transwell migration assay

The migration of HT-29 cells in a 3D condition (spheroids) was evaluated using a Transwell migration assay. To this end, Transwell chambers with 8.0 μm pore polycarbonate membrane inserts (Corning Inc.; Corning, NY, USA) were used. After the treatment of HT-29 spheroids with Gemini-Cur NPs, a single-cell suspension was made using the Trypsin–EDTA solution. Then, 200 μl of serum-free medium containing 2×10^4 cells was transferred into inserted. The basolateral chamber was filled with 700 μl of culture medium enriched with 1–2% FBS. Plates were kept at 37 °C for 24 h. Thereafter, the number of migrated cells at the bottom surface was counted in 5 random fields. To better identify the migrated cells at the bottom of the plates, we fixed the cells with precooled methanol solution for 10 min and stained with Giemsa solution (Sigma-Aldrich; St. Louis, MO).

Real-time PCR assay

Total RNA was extracted from both of the control and treated HT-29 spheroids using TRIzol™ reagent (Bioneer, Korea) according to the manufacturer's guideline. The quality and concentration of RNAs were determined using a Picodrop spectrophotometer (Thermo) and 1% agarose gel electrophoresis. Easy™cDNA Synthesis Kit (Parstous Company, IRAN) was used to synthesize cDNA by the oligo-dT method following the manufacturer's instructions. The expression of genes related to epithelial-mesenchymal transition (EMT), such as E-cadherin and Vimentin, was evaluated using real-time PCR analysis. The reaction was performed by SYBR Green (AMPLIQON, Denmark) and appropriate primers. The primers were designed using Oligo7 software (Table 1). In this study, the total volume for real-time PCR reaction reached 10 μl consisted of 5 μl of SYBR Green PCR master mix, 1 μl of forward and reverse primers, 1 μl of cDNA template, and 3 μl of ddH_2O. Relative gene expression was normalized to GAPDH as an internal control, and calculated by using the $2^{-\Delta\Delta CT}$ method.

Table 1 Primer list

Gene	Sequence (5′ → 3′)	T^m (°C)
Vimentin	*F*: 5′-GAGGAAGCCGAAAACACCCT-3′ *R*: 5′-AGATTCCACTTTGCGTTCAAGG-3′	59
E-cadherin	*F*: 5′-GAACACATTTGCCCAATTCCA-3′ *R*: 5′-CCTACCCCTCAACTAACCC-3′	59

Western blotting

After treatment with Gemini-Cur NPs, cells were lysed using 500 µl of lysis buffer (Tris–HCl pH 8, 0.08 g NaCl, 0.003 g EDTA, 0.025 g Sodium Deoxycholate, 0.01 g SDS, and 1% NP40 enriched with an anti-protease cocktail). Thereafter, 10 µg of protein from each group was electrophoresed using 10% SDS-PAGE at 120 V for 45 min and then transferred onto polyvinylidene difluoride membranes at 120 V for 1.5 h. Membranes were incubated with appropriate primary antibodies, including E-cadherin (Cat no; sc-21791; Santa Cruz Biotechnology, Inc.), Vimentin (Cat no: 14-9897-82; Thermo Fisher Scientific), MMP-2 (Cat no: sc-10736; Santa Cruz Biotechnology, Inc.), and MMP-9 (Cat no: sc-393859; Santa Cruz Biotechnology, Inc.), at 4 °C overnight. After three-time PBS wash, the membranes were incubated with appropriate HRP-conjugated secondary antibodies (Cat no: sc-516102 and sc-2357; Santa Cruz Biotechnology, Inc.) for 1 h at room temperature. The immunoblots were detected on X-ray films using chemiluminescence ECL solution (Bio-Rad). β-actin (Cat no: sc-47778; Santa Cruz Biotechnology, Inc.) is considered as a housekeeping protein to normalize the protein level of different factors.

Results

FTIR analysis confirmed successful conjugation of Cur to Gemini NPs

The Gemini-Cur NPs FTIR analysis revealed respective peaks at the wavelengths of 2895 and 1115 cm^{-1} which are related to C–H and C–O stretching, respectively. These peaks were detectable in Gemini NPs. The analysis showed the increase of C–H stretching in Gemini-Cur NPs compared to Gemini NPs. The conjugation of Cur to Gemini NPs increased C=O and O–H bonds (Fig. 1a).

SEM analysis and uptake test

SEM analysis revealed nearly round-shape Cur + Gemini NPs reaching 120.3 ± 20.43 nm (Fig. 1b). Based on data from IF imaging, we found that HT-29 cells could successfully uptake the Cur + Gemini NPs in which stronger intracellular fluorescence signals were detected inside the cells after a 6-h incubation of HT-29 cells with Cur + Gemini NPs (Fig. 1c). In addition to intracellular fluorescence appearance, we found membrane-bounded NPs in groups treated with Cur + Gemini NPs and Cur. Interestingly, the binding of curcumin to cell membrane shows a weak cellular uptake compared to the Gemini-Cur NPs. As expected, no fluorescence activity was obtained in control and Gemini surfactant groups. These data confirmed that Gemini surfactant NPs enhanced the water solubility of Cur, leading to appropriate uptake in human HT-29 cells.

Gemini-Cur NPs decreased the viability of HT-29 in a 2D culture system

To evaluate the possible cytotoxic effect of Gemini-Cur NPs on HT-29 cells in a 2D culture system, MTT assay was performed by using different concentrations of Gemini-Cur NPs, including 20, 60, 100, 200, 300, 400, 500, 600, 700,800, and 900 µM (Fig. 2a). Data showed that the viability of the HT-29 cell was reduced 48 h after being exposed to different doses of Gemini-Cur NPs in a dose-dependent manner compared to the control group ($p < 0.001$). We found a slight reduction in the viability of cells from group 20 µM Gemini-Cur NPs in comparison with the non-treated

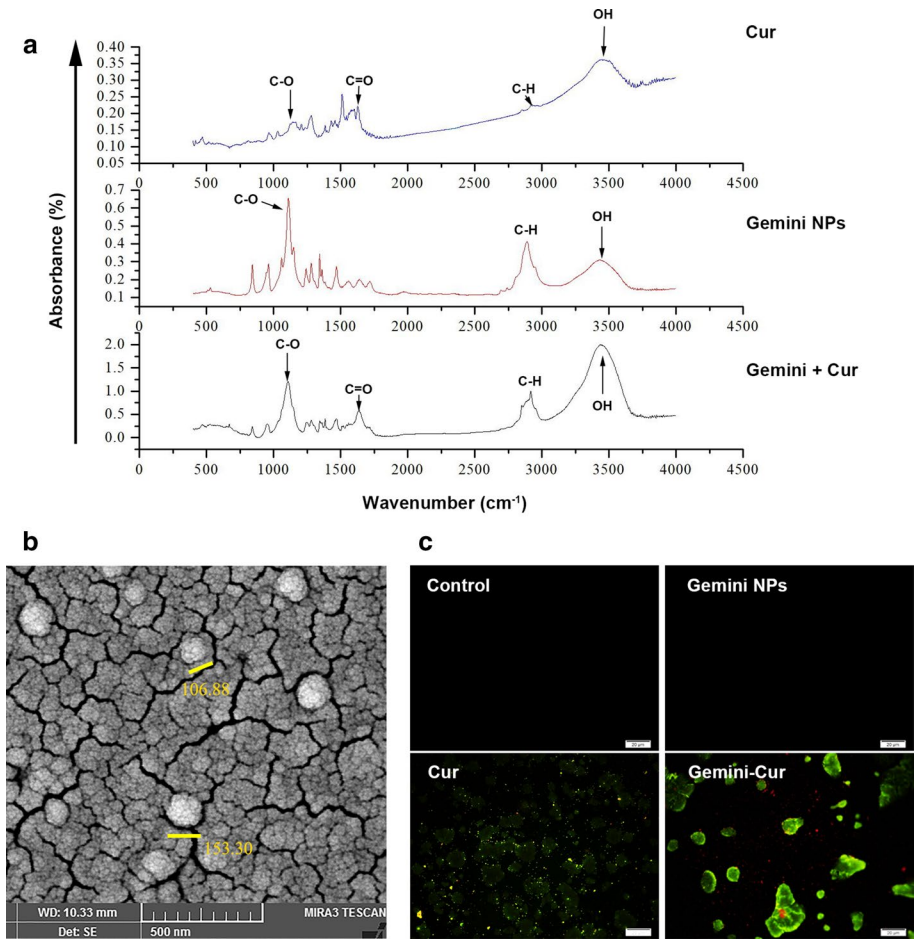

Fig. 1 FTIR analysis (**a**), SEM imaging (**b**), and uptake of Gemini-Cur NPs after 6 h (**c**). A subcellular accumulation of Gemini-Cur NPs was found in human colorectal adenocarcinoma HT-29 cells compared to the group incubated with the Cur alone

cells ($p > 0.05$; Fig. 2a). By increasing the concentration of Gemini-Cur NPs to 60 μM, we recorded ~ 22% in cell viability and this value reached 42% in the group received 100 μM NPs. Data showed the maximum tumoricidal effect of Gemini-Cur NPs in doses above 100 μM NPs in which the viability of cells reached near to 20% of non-treated cells in the group exposed to 200 μM NPs (Fig. 2a). According to statistical analysis, we found non-significant differences in cell survival rate between groups that received doses above 200 μM NPs. According to MTT data, we found that the IC50 for Gemini-Cur NPs against HT-29 cells was 80 μM.

Gemini-Cur NPs increased HT-29 tumoroid diameter by decreasing structural consistency

It is believed that 3D cell culture and tumoroid formation can imitate in part, but not completely, the in vivo behavior of cancer cells as seen inside the tumor stroma. Here, we developed tumoroid aggregates of HT-29 to assess whether Gemini-Cur NPs could penetrate the 3D tumor structure and compare the result with the 2D culture system. To assess the feasible role of Gemini-Cur NPs on the diameter of HT-29 spheroids, we performed a 3D culture system. Based on obtained data, the diameter

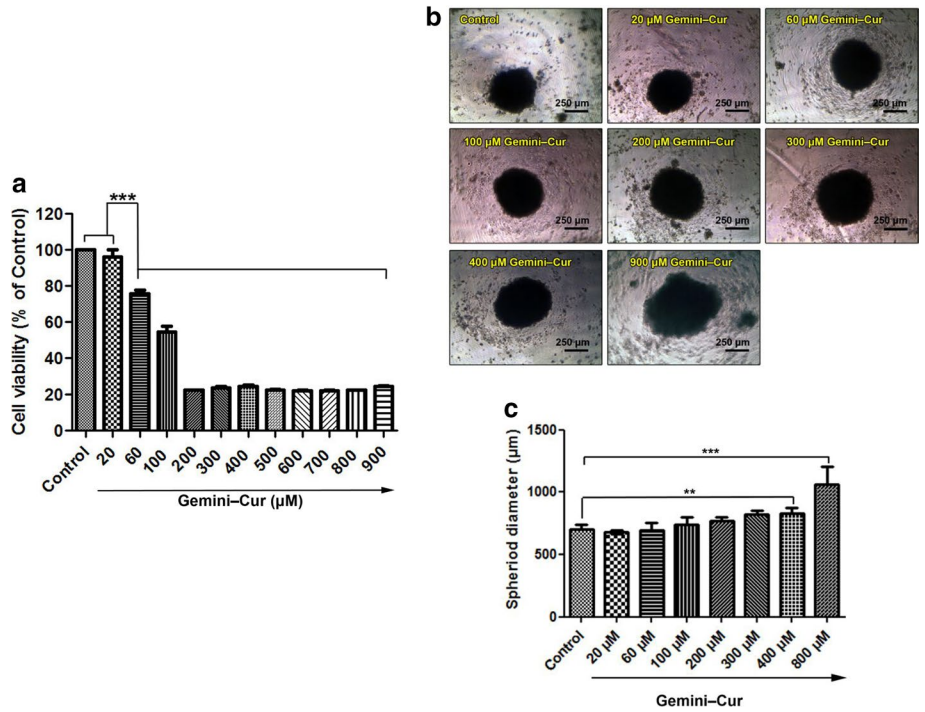

Fig. 2 Measuring the viability of HT-29 cells using MTT assay in a 2D culture system after 48 h ($n = 8$; **a**). Data showed that the viability of HT-29 cells was decreased by increasing the concentration of Gemini-Cur NPs. In this assay, the incubation of HT-29 cells with 60 μM and higher doses significantly decreases the viability of cells compared to the non-treated control cells. Evaluation of Gemini-Cur NPs on HT-29 cell spheroids after 48 h (**b**, **c**). Bright-field imaging showed the ability of HT-29 cells to generate spheroids by the hanging drop method. The incubation of spheroids with different doses of Gemini-Cur NPs contributed to the loss of spheroid integrity and structure. By increasing the dose of Gemini-Cur NPs, the diameter of spheroids was significantly increased and yielded a loose appearance ($n = 5$). We found statistically significant differences in the diameter of spheroids treated with 400 and 800 μM Gemini-Cur compared to the control cells. One-way ANOVA with Tukey post hoc analysis. $^{**}p < 0.01$; $^{***}p < 0.001$

of spheroids increased along with the increase of Gemini-Cur NPs concentration in which the mean diameter of spheroids in groups 400 and 800 μM was significantly increased compared to the non-treated control cells (Fig. 2b, c; $p < 0.01$ and $p < 0.001$). In the presence of Gemini-Cur NPs, spheroids began to disintegrate and lose central density after 48 h. One reason would be that the Gemini-Cur NPs could appropriately penetrate the tumoroid structure supporting the loss of cell adhesion which in turn contributed to the efficient distribution of these NPs to deeper layers. These data demonstrated that the exposure of HT-29 tumoroid cells to the Gemini-Cur NPs weakens the structural consistency and integrity and contributes to a decrease of cell-to-cell connection and intercellular connectivity.

Gemini-Cur NPs decreased the viability of HT29 tumoroid cells

The viability of cells inside tumoroids was evaluated using LDH released to the supernatant 48 h after being treated with different doses of Gemini-Cur NPs, indicating the membrane integrity. Data showed that the released LDH contents were increased in

groups treated with Gemini-Cur NPs compared to the control cells ($p < 0.05$: Fig. 3a). In the control group, LDH activity was about 0.025 IU/l, whereas following the treatment process, we found an upward trend by increasing Gemini-Cur NPs concentration. In group 400 µM Gemini-Cur NPs, we found maximum levels of LDH that show the highest toxicity compared to all groups ($p < 0.05$; Fig. 3a). These data showed that the integrity of HT-29 cells was interrupted in the presence of Gemini-Cur NPs and these effects are closely associated with the increase of Gemini-Cur NPs concentration.

Analyzing Gemini-Cur NPs penetration into tumoroids using flow cytometry

Owing to the fluorescent entity of Gemini-Cur NPs, penetration and uptake could be done based on the fluorescence-based assays (Fig. 3b). The cellular uptake of Gemini-Cur NPs was studied via flow cytometry technique after 48 h. Based on the data, the fluorescence rate was $3.02 \pm 0.3\%$ after treatment of cells with 80 µM Gemini-Cur NPs, while this value reached $16.91 \pm 4.3\%$ in the group received 300 µM Gemini-Cur NPs (Fig. 3b). It should be noted that the level of fluorescent intensity in cells

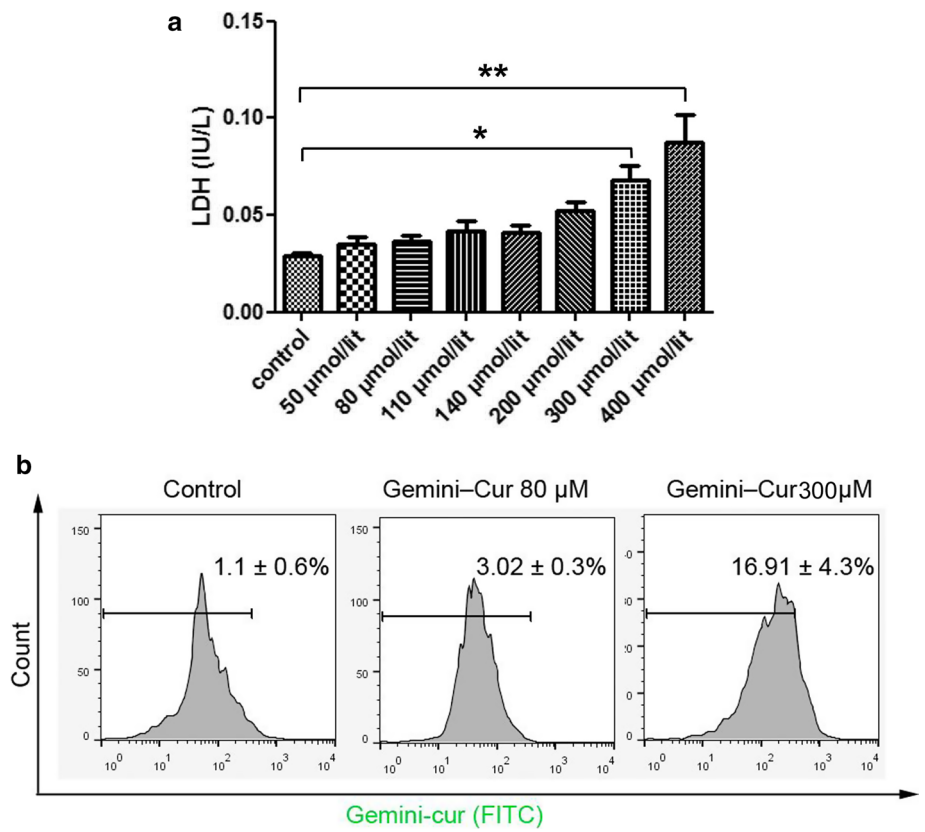

Fig. 3 Measuring the 3D spheroid HT-29 cells viability by LDH release after 48 h (**a**; $n = 3$). The incubation of HT-29 cell spheroids with Gemini-Cur NPs increased the release of LDH to the supernatant, indicating the loss of membrane integrity after being exposed to the Gemini-Cur NPs in vitro ($n = 3$). The uptake of Gemini-Cur NPs by 3D spheroid HT-29 cells was evaluated using flow cytometry analysis (**b**; $n = 3$). By increasing the Gemini-Cur NPs from 80 to 300 µM, the intracellular fluorescence was increased, showing the close relationship between Gemini-Cur NP concentration and fluorescence intensity. One-way ANOVA with Tukey post hoc analysis. *$p < 0.05$; *** $p < 0.01$

of tumoroids relied on the initial concentration of Gemini-Cur NPs and the loss of microaggregate integrity.

Treatment of HT-29 tumoroid cells with Gemini-Cur NPs decreased Rhodamin123 efflux capacity

To examine the effect of Gemini-Cur NPs on MDR activity, we used Rhodamine efflux capacity via flow cytometry analysis (Fig. 4a). Data showed that Rhodamine 123-positive cells were $20.1 \pm 2.4\%$ in control cells. Compared to non-treated cells, the exposure of cells to 80 and 300 µM Gemini-Cur NPs increased significantly the percent of Rhodamine 123-positive cells to 40.8 ± 3.04 ($p < 0.05$) and $52.0 \pm 6.3\%$ ($p < 0.01$), respectively (Fig. 4a). These data showed that Gemini-Cur NPs could inhibit the normal function of MDR proteins in a dose-dependent manner.

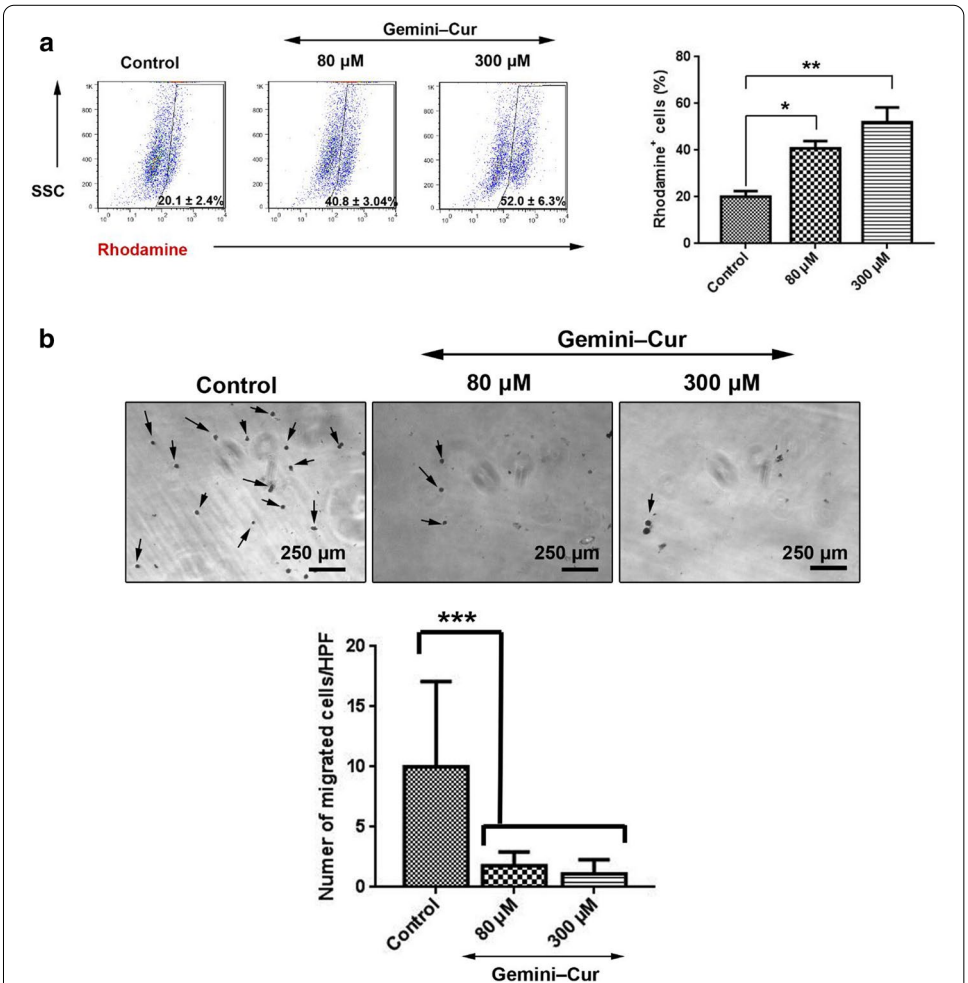

Fig. 4 The Rhodamine 123 efflux assay (**a**). Flow cytometry analysis revealed the loss of Rhodamine 123 efflux capacity in 3D spheroid HT-29 cells after 48 h of incubation with Gemini-Cur NPs. The cells lost Rhodamine 123 efflux capacity after being treated with Gemini-Cur NPs in a dose-dependent manner. Analysis of cell migration by Transwell inserts assay (**b**). The migration of 3D spheroid HT-29 cells was decreased upon treatment with 80 and 300 Gemini-Cur NPs after 48 h, indicating the inhibition of cell migration in a 3D culture system exposed to Gemini-Cur NPs

Gemini-Cur NPs inhibited the migration of HT-29 tumoroid cells

We used a Transwell cell migration assay to assess the possible impact of Gemini-Cur NPs on HT-29 tumoroid cells (Fig. 4b). Following 48-h treatment, we found a magnificent decrease in the number of Gemini-Cur NP-treated HT-29 cells compared to the control group ($p < 0.05$; Fig. 4b). We found that the treatment of tumoroids with 80 and 300 μM Gemini-Cur NPs decreased the number of migrated cells at the basolateral surface of plates compared to the control group ($p < 0.001$; Fig. 4b). Along with this assay, we also performed Western blotting to measure the protein levels of MMP-2 and MMP-9 in tumoroid cells after being treated with 80 and 300 μM Gemini-Cur NPs (Fig. 5a, b). Data showed that the protein levels of MMP-2 and -9 were significantly decreased in the 300 μM Gemini-Cur NPs group compared to the control cells ($p < 0.05$ and $p < 0.01$; Fig. 5a, b). Despite the decrease of MMP-2 and -9 levels in group 80 μM Gemini-Cur NPs, we found a non-significant difference in comparison with control cells. These data showed that Gemini-Cur NPs could inhibit the migration of HT-29 cells in tumoroid structure via suppression of MMPs, especially in higher doses.

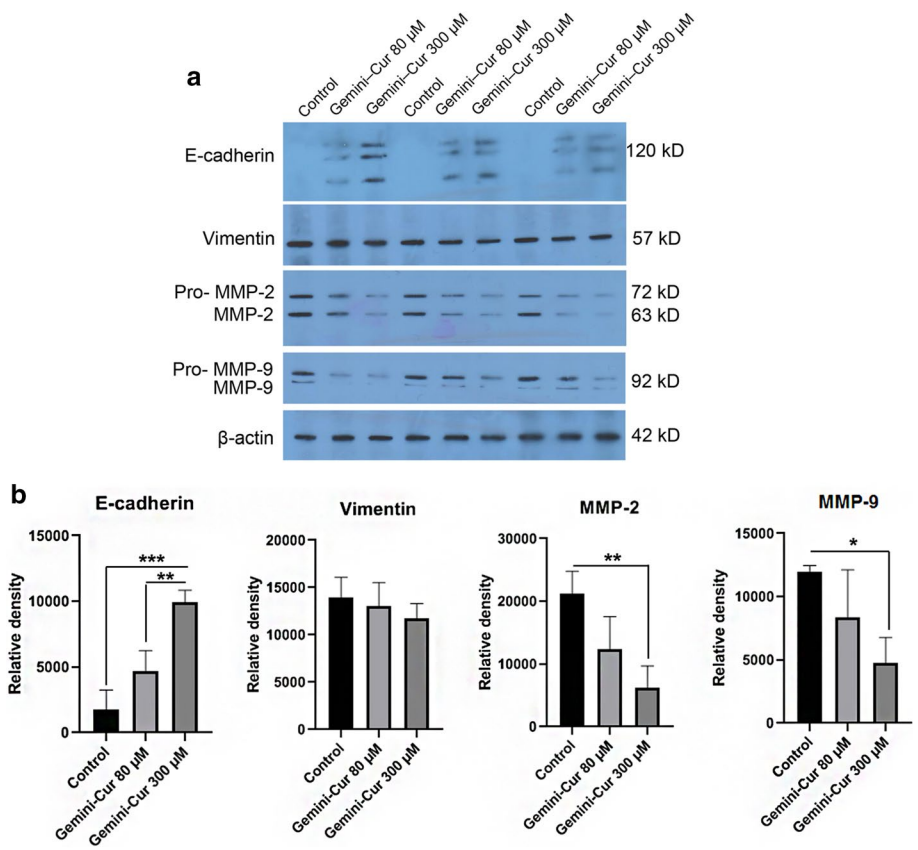

Fig. 5 Measuring protein levels of MMP-2 and MMP-9 and EMT rate in 3D spheroid HT-29 cells using Western blotting after 48 h ($n = 3$). Data showed the significant decrease of cell metastasis indicated by the suppression of MMP-2 and -9. The incubation of spheroids with 80 and 300 μM Gemini-Cur NPs decreased EMT rate indicated with reduced Vimentin and increased E-cadherin levels compared to the control group. Protein levels of Vimentin were not significantly altered after being exposed to 80 and 300 μM Gemini-Cur NPs. One-way ANOVA with Tukey post hoc analysis. * $p < 0.05$; ** $p < 0.01$; *** $p < 0.01$

Gemini-Cur NPs altered EMT capacity in HT-29 tumoroid cells

To this end, the expression and protein levels of factors participating in the EMT process were evaluated using Western blotting and real-time PCR analyses. Western blotting showed that the treatment of HT-29 tumoroid cells with 80 and 300 µM Gemini-Cur NPs altered the protein levels of E-cadherin compared to the control cells (Fig. 5a, b). Based on the data, the protein levels of E-cadherin were increased in HT-29 tumoroid cells upon treatment with 80 ($p < 0.01$) and 300 µM ($p < 0.001$) Gemini-Cur NPs compared to the control group. Despite the reduction in the protein value of Vimentin, these values did not contribute statistically significant differences ($p > 0.05$; Fig. 5a, b). The expression of *E-cadherin* and *Vimentin* genes was also analyzed by real-time PCR assay (Fig. 6). Concerning real-time PCR analysis, the fold change of *E-cadherin* gene expression was statistically non-significant in cells received 80 and 300 µM Gemini-Cur NPs compared to the control cells ($p > 0.05$). Based on our data, Vimentin expression was diminished significantly in group 300 µM Gemini-Cur NPs compared to the control ($p > 0.01$). However, the changes in the group with 80 µM Gemini-Cur NPs were not statistically significant compared to the control non-treated cells. These data showed that the treatment of HT-29 tumoroid cells with Gemini-Cur NPs could alter the EMT phenomenon and decrease the cell resistance and decreased the stemness feature inside the tumor niche.

Discussion

The CRC consists of a very heterogeneous group of anaplastic changes making it resistant to common medications in the clinical setting (Rawla et al. 2019). Turning to the most common therapies, such as surgical approaches, chemotherapeutic agents, radiotherapy, and hormone medication, shows that these therapeutic policies would not usually work for a prolonged period and possibly put patients in trouble due to

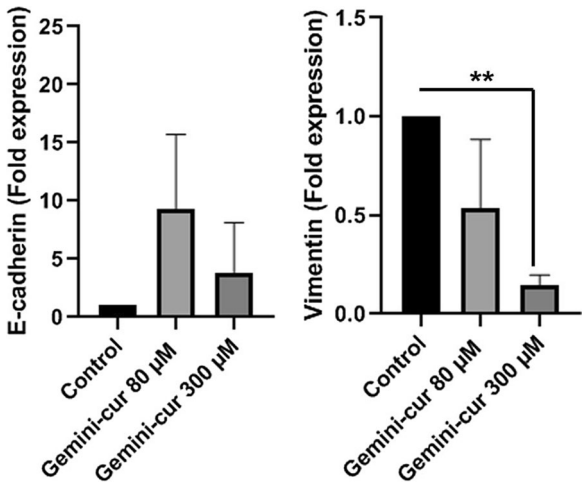

Fig. 6 Measuring the expression of Vimentin and E-cadherin by real-time PCR analysis ($n = 3$). Data showed the increase of E-cadherin and decrease of Vimentin showing the suppression of stemness and phenotype shifting in 3D spheroid HT-29 cells after 48 h of incubation with Gemini-Cur NPs. One-way ANOVA with Tukey post hoc analysis. ** $p < 0.01$

wide ranges of side effects (Rawla et al. 2019; Arruebo et al. 2011). In the current study, we aimed to highlight the tumoricidal properties of Gemini-Cur NPs in human colorectal carcinoma cell spheroids after 48 h in vitro.

Based on our data, Gemini-Cur NPs induced cell-specific responses in the 2D culture system indicated by a reduced survival rate in a dose-dependent manner. Consistent with the current data, Song and co-workers previously proved the tumoricidal effect of Cur on human HT-29 cells in a dose- and time-dependent manner via the promotion of pro-apoptotic factors, such as p53, Bax, Caspase 3, and Caspase 9, and suppression of anti-apoptotic factors, such as Bcl-2 (Song et al. 2005). Previously, our group showed that the treatment of breast cancer cells with Gemini-Cur NPs contributed to magnificent cell death via the inhibition of cell proliferation and the promotion of apoptosis (Karimpour et al. 2019). Concerning the hydrophobic nature of Cur and the low distribution rate, major drawbacks still limit the tumoricidal effects of this phytocompound inside the body (Nayak et al. 2016). Also, we designated 3D cancer spheroids to mimic structural and functional in vivo human solid tumors. According to our data, in the culture medium enriched with increasing concentrations of Gemini-Cur NPs, spheroids began to disintegrate and lose central density after 48 h. The rising supernatant LDH along with the increase in diameter of HT-29 spheroids highlights the efficient penetration of Gemini-Cur NPs and the induction of cell death. To show effective penetration and absorption of Gemini-Cur NPs, the fluorescence intensity of HT-29 spheroids was investigated using flow cytometry analysis. By increasing the concentration of Gemini-Cur NPs, large amounts of cells became fluorescent, indicating enhanced NPs uptake. In support of these data, it should be noted that the application of high-dose Gemini-Cur NPs (300 μM) in 3D tumor culture may improve cancer cell death in the outer cell layers by promoting the loss of cell adhesion which in turn contributed to the efficient distribution of these NPs to deeper layers.

An increase in fluorescence intensity and accumulation of Rhodamine 123 is associated with mitochondrial dysfunction and loss of MDR-dependent drug resistance (Twentyman et al. 1994). Consistent with our data, Gemini-Cur NPs decreased the ability of cancer cells in 3D structure to efflux Rhodamine 123 in a dose-dependent manner, indicating the gradual inhibition of MDR-dependent drug resistance.

The exposure of HT-29 cell spheroids to Gemini-Cur NPs reduced the migration rate in the Transwell insert system. It has been shown that the inhibition of cancer cell migration is done via the inhibition of signaling pathways, such as TGF-β/Smad and Akt/SKP2 signaling pathways (Vutakuri 2018). In support of these data, we noted the decrease of MMP-2 and MMP-9 in spheroids treated with Gemini-Cur NPs compared to the control group. It has been shown that Cur inhibited lung cancer cell metastasis via attenuating GLUT1/MT1-MMP/MMP2 pathway (Liao et al. 2015). It seems that the incubation of HT-29 spheroids with Gemini-Cur NPs could inhibit the activity of intracellular signaling pathways and the production of degrading enzymes, such as MMPs.

The promotion of EMT is touted as one of the mechanisms that contributed to tumor resistance against different chemotherapeutic agents (Pouyafar et al. 2019). According to our data, the incubation of HT-29 spheroids with Gemini-Cur NPs increased mesenchymal-to-epithelial transition via the increase of E-cadherin and suppression of

stemness-related factors, namely Vimentin. In line with our data, Aedo-Aguilera et al. found that the treatment of cervical cancer cells with Cur decreased EMT indicated with increased E- and N-cadherin via the Pirin-dependent mechanism (Aedo-Aguilera et al. 2019). The increase of epithelial-like phenotype in tumor cell aggregates decreases the possibility of stemness features and resistance to chemotherapeutic agents. One of the most advantages of Gemini surfactants-based drug delivery is the property of Gemini surfactant to self-assemble into nanoparticles in different morphological structures, like liposomes, cubosomes, micelles, and inverted micelles to harbor small and large sizes to the host cells (Singh et al. 2015). Preliminary data showed the eligibility of Gemini surfactant-based NPs to deliver monoclonal antibody Fab fragment to melanoma cells in a mouse xenograft model (Makhlouf et al. 2019). Whether this delivery system could be efficient in in vivo system to deliver drug and therapeutic agents to the deep layers of tissues remains a matter of debate. Attempts should be focused to assess the kinetics of Gemini surfactants-based NPs in the systemic circulation and local target sites.

Conclusions

The current experiment highlighted the tumoricidal effect of Cur on HT-29 cell spheroids, which mimics the in vivo condition. Cur is the potential to suppress tumor cell activity and functional behavior via different mechanisms.

Acknowledgements
The authors appreciate the personnel of Stem Cell Research Center for help and guide.

Authors' contributions
ZZ, ARNZ and HJA performed experiments and prepared draft. EB and RR designed and supervised the study. All the authors read and approved the final manuscript.

Funding
This study was originated from an MSc thesis and supported by a Grant from the University of Tabriz and Tabriz University of Medical Sciences (IR.TBZMED.VCR.REC.1399.189).

Availability of data and materials
The datasets used and/or analyzed during the current study are available from the corresponding author on reasonable request.

Ethics approval and consent to participate
Not applicable.

Consent for publication
Not applicable.

Competing interests
The authors declare there is no conflict of interest in this study.

Author details
[1] Department of Animal Biology, School of Natural Sciences, University of Tabriz, Tabriz 51555, Iran. [2] Institute of Environment, University of Tabriz, Tabriz, Iran. [3] Stem Cell Research Center, Tabriz University of Medical Sciences, Tabriz, Iran. [4] Department of Applied Cell Sciences, Faculty of Advanced Medical Sciences, Tabriz University of Medical Sciences, Golgasht St., Tabriz 5166614756, Iran.

Received: 8 October 2020 Accepted: 24 December 2020
Published online: 06 January 2021

References

Abdolahinia ED, Nadri S, Rahbarghazi R, Barar J, Aghanejad A, Omidi Y. Enhanced penetration and cytotoxicity of metformin and collagenase conjugated gold nanoparticles in breast cancer spheroids. Life Sci. 2019;231:116545.
Aedo-Aguilera V, Carrillo-Beltrán D, Calaf GM, Muñoz JP, Guerrero N, Osorio JC, Tapia JC, León O, Contreras HR, Aguayo F. Curcumin decreases epithelial-mesenchymal transition by a Pirin-dependent mechanism in cervical cancer cells. Oncol Rep. 2019;42(5):2139–48.

Aleandri S, Bombelli C, Bonicelli MG, Bordi F, Giansanti L, Mancini G, Ierino M. Sennato S (2013) Fusion of gemini based cationic liposomes with cell membrane models: implications for their biological activity. Biochimica et Biophysica Acta. 1828;2:382–90. https://doi.org/10.1016/j.bbamem.2012.10.001.
Arruebo M, Vilaboa N, Sáez-Gutierrez B, Lambea J, Tres A, Valladares M, González-Fernández Á. Assessment of the evolution of cancer treatment therapies. Cancers. 2011;3(3):3279–330.
Chaudhary T, Chahar A, Sharma JK, Kaur K, Dang A. Phytomedicine in the treatment of cancer: a health technology assessment. J Clin Diagn Res. 2015;9(12):XC04.
Chauhan PS, Singh DK, Dash D, Singh R. Intranasal curcumin regulates chronic asthma in mice by modulating NF-κB activation and MAPK signaling. Phytomedicine. 2018;51:29–38. https://doi.org/10.1016/j.phymed.2018.06.022.
Cheraghi O, Dehghan G, Mahdavi M, Rahbarghazi R, Rezabakhsh A, Charoudeh HN, Iranshahi M, Montazersaheb S. Potent anti-angiogenic and cytotoxic effect of conferone on human colorectal adenocarcinoma HT-29 cells. Phytomedicine. 2016;23(4):398–405. https://doi.org/10.1016/j.phymed.2016.01.015.
Du J, Chen Q, Liu Q, Hu X (2018) Synthesis of a novel Gemini cationic surfactant and its inhibition behaviour and mechanism study on 2024 Al-Cu-Mg alloy in acid solution. International Journal of Corrosion 2018
Hewlings SJ, Kalman DS. Curcumin: a review of its effects on human health. Foods. 2017;6(10):92.
Karimpour M, Feizi MAH, Mahdavi M, Krammer B, Verwanger T, Najafi F, Babaei E. Development of curcumin-loaded gemini surfactant nanoparticles: synthesis, characterization and evaluation of anticancer activity against human breast cancer cell lines. Phytomedicine. 2019;57:183–90.
Lee W-H, Loo C-Y, Bebawy M, Luk F, Mason RS, Rohanizadeh R. Curcumin and its derivatives: their application in neuropharmacology and neuroscience in the 21st century. Curr Neuropharmacol. 2013;11(4):338–78.
Liao H, Wang Z, Deng Z, Ren H, Li X. Curcumin inhibits lung cancer invasion and metastasis by attenuating GLUT1/MT1-MMP/MMP2 pathway. Int J Clin Exp Med. 2015;8(6):8948.
Makhlouf A, Hajdu I, Hartimath SV, Alizadeh E, Wharton K, Wasan KM, Badea I, Fonge H. 111In-Labeled Glycoprotein Nonmetastatic b (GPNMB) targeted gemini surfactant-based nanoparticles against melanoma: in vitro characterization and in vivo evaluation in melanoma mouse xenograft model. Mol Pharm. 2019;16(2):542–51. https://doi.org/10.1021/acs.molpharmaceut.8b00831.
Nayak AP, Mills T, Norton I. Lipid Based Nanosystems for Curcumin: Past, Present and Future. Curr Pharm Des. 2016;22(27):4247–56.
Nunes AS, Barros AS, Costa EC, Moreira AF, Correia IJ. 3D tumor spheroids as in vitro models to mimic in vivo human solid tumors resistance to therapeutic drugs. Biotechnol Bioeng. 2019;116(1):206–26. https://doi.org/10.1002/bit.26845.
Pouyafar A, Rezabakhsh A, Rahbarghazi R, Heydarabad MZ, Shokrollahi E, Sokullu E, Khaksar M, Nourazarian A, Avci ÇB. Treatment of cancer stem cells from human colon adenocarcinoma cell line HT-29 with resveratrol and sulindac induced mesenchymal-endothelial transition rate. Cell Tissue Res. 2019;376(3):377–88.
Pretzsch E, Bösch F, Neumann J, Ganschow P, Bazhin A, Guba M, Werner J, Angele M. Mechanisms of Metastasis in Colorectal Cancer and Metastatic Organotropism: Hematogenous versus Peritoneal Spread. Journal of oncology. 2019;2019:7407190.
Rahimi HR, Nedaeinia R, Shamloo AS, Nikdoust S, Oskuee RK. Novel delivery system for natural products: nano-curcumin formulations. Avicenna J Phytomed. 2016;6(4):383.
Rahnavard M, Hassanpour M, Ahmadi M, Heidarzadeh M, Amini H, Javanmard MZ, Nouri M, Rahbarghazi R, Safaie N. Curcumin ameliorated myocardial infarction by inhibition of cardiotoxicity in the rat model. J Cell Biochem. 2019;120(7):11965–72.
Rawla P, Sunkara T, Barsouk A. Epidemiology of colorectal cancer: Incidence, mortality, survival, and risk factors. Przegląd Gastroenterologiczny. 2019;14(2):89.
Sebak A. Limitations of PEGylated nanocarriers: unfavourable physicochemical properties, biodistribution patterns and cellular and subcellular fates. Int J Pharm. 2018;10:6–12.
Shome S, Talukdar AD, Choudhury MD, Bhattacharya MK, Upadhyaya H. Curcumin as potential therapeutic natural product: a nanobiotechnological perspective. J Pharm Pharmacol. 2016;68(12):1481–500.
Singh J, Michel D, Getson HM, Chitanda JM, Verrall RE, Badea I. Development of amino acid substituted gemini surfactant-based mucoadhesive gene delivery systems for potential use as noninvasive vaginal genetic vaccination. Nanomedicine. 2015;10(3):405–17. https://doi.org/10.2217/nnm.14.123.
Song G, Mao Y, Cai Q, Yao L, Ouyang G, Bao S. Curcumin induces human HT-29 colon adenocarcinoma cell apoptosis by activating p53 and regulating apoptosis-related protein expression. Braz J Med Biol Res. 2005;38(12):1791–8.
Srivastava NS, Srivastava RAK. Curcumin and quercetin synergistically inhibit cancer cell proliferation in multiple cancer cells and modulate Wnt/β-catenin signaling and apoptotic pathways in A375 cells. Phytomedicine. 2019;52:117–28. https://doi.org/10.1016/j.phymed.2018.09.224.
Twentyman PR, Rhodes T, Rayner S. A comparison of rhodamine 123 accumulation and efflux in cells with P-glycoprotein-mediated and MRP-associated multidrug resistance phenotypes. Eur J Cancer. 1994;30(9):1360–9.
Vallianou NG, Evangelopoulos A, Schizas N, Kazazis C. Potential anticancer properties and mechanisms of action of curcumin. Anticancer Res. 2015;35(2):645–51.
Vutakuri N (2018) Curcumin-breast cancer therapeutic agent to replace allopathic treatments with extensive side effects. J Young Investig 35 (2)
Wang J-b, Qi L-l, Wu T-x. Curcumin induces apoptosis through the mitochondria-mediated apoptotic pathway in HT-29 cells. J Zhejiang Univ Sci B. 2009;10(2):93–102.
Wang M, Jiang S, Zhou L, Yu F, Ding H, Li P, Zhou M, Wang K. Potential mechanisms of action of curcumin for cancer prevention: focus on cellular signaling pathways and miRNAs. Int J Biol Scis. 2019;15(6):1200.

Publisher's Note